Published in final edited form as:
Mol Pharm. 2010 December 6; 7(6): 1930–1939. doi:10.1021/mp100221h.

pH-sensitive siRNA Nanovector for Targeted Gene Silencing and Cytotoxic Effect in Cancer Cells

Hyejung Mok[1], **Omid Veiseh**[1], **Chen Fang**[1], **Forrest M. Kievit**[1], **Freddy Y. Wang**[1], **James O. Park**[2], and **Miqin Zhang**[*,1,3,4]

[1]Department of Materials Science and Engineering, University of Washington, Seattle, WA 98195 USA

[2]Department of Surgery, University of Washington, Seattle, WA 98195 USA

[3]Department of Radiology, University of Washington, Seattle, WA 98195 USA

[4]Department of Neurological Surgery, University of Washington, Seattle, WA 98195 USA

Abstract

A small interfering RNA (siRNA) nanovector with dual targeting specificity and dual therapeutic effect is developed for targeted cancer imaging and therapy. The nanovector is comprised of an iron oxide magnetic nanoparticle core coated with three different functional molecules: polyethyleneimine (PEI), siRNA, and chlorotoxin (CTX). The primary amine group of PEI is blocked with citraconic anhydride that is removable at acidic conditions, not only to increase its biocompatibility at physiological conditions but also to elicit a pH-sensitive cytotoxic effect in the acidic tumor microenvironment. The PEI is covalently immobilized on the nanovector via a disulfide linkage that is cleavable after cellular internalization of the nanovector. CTX as a tumor-specific targeting ligand and siRNA as a therapeutic payload are conjugated on the nanovector via a flexible and hydrophilic PEG linker for targeted gene silencing in cancer cells. With a size of ~ 60 nm, the nanovector exhibits long-term stability and good magnetic property for magnetic resonance imaging. The multifunctional nanovector exhibits both significant cytotoxic and gene silencing effects at acidic pH conditions for C6 glioma cells, but not at physiological pH conditions. Our results suggest that this nanovector system could be safely used as a potential therapeutic agent for targeted treatment of glioma as well as other cancers.

Keywords

siRNA; iron oxide nanoparticle; cytotoxicity; pH-sensitive; cancer; nanotechnology

1. Introduction

RNA interference (RNAi) using small interfering RNA (siRNA), a 19–21 base pair double stranded RNA, has been touted as a potential therapeutic breakthrough for genetic disorders such as cancers by specific and efficient target-gene inhibition.1⁻2 An effective delivery vector system that can accommodate the highly negative charge and rigid structure of siRNAs, but also ensure efficient processing through endosomal escape remains an essential yet challenging component for successful clinical application of RNAi. Inorganic nanoparticles, including quantum dots, gold nanoparticles, and iron oxide nanoparticles with

[*]Corresponding author: Department of Materials Science and Engineering, University of Washington, Seattle WA 98195 USA; Telephone: 206 616 9356; Fax: 206 543 3100; mzhang@u.washington.edu.

siRNAs directly conjugated by covalent bonds or by physical adsorption onto their surfaces have been studied as siRNA carriers.[3–6] Of these, biodegradable superparamagnetic iron oxide nanoparticles (NPs) are an attractive option, as they afford efficient delivery of siRNA *in vitro* and *in vivo* with minimal toxicity, but also endow the added benefit of localization using magnetic resonance (MR) imaging.[4,7–9] Surface modifications of NPs with polymers such as polyethylenimine (PEI), poly-L-lysine (PLL), and polyethylene glycol (PEG) increase intracellular delivery of these NPs as well as improve their stability and circulation time.[4,8,10–12] PEI is a well-characterized and commercialized cationic polymer with a high charge density, one protonable nitrogen per every third atom. PEI has been widely used as a coating material of inorganic nanoparticles as well as a carrier itself for gene delivery because of its strong electrostatic affinity to nucleotides as well as efficient endosomal escape via the proton sponge effect after intracellular uptake.[13–15] However, its nonspecific cytotoxicity caused by destabilization of cellular and mitochondrial membranes and activation of intracellular apoptotic signals limit its clinical application.[16–18] Various chemical modifications to reduce its nonspecific cytotoxicity while maintaining its superior gene delivery efficiency, using small molecules, natural polymers, and peptides, have been vigorously investigated.[8,13,19–21] Citraconic anhydride (2-methylmaleic anhydride), a derivative of maleic anhydride, reacts with primary amine groups, resulting in amide linkages with terminal carboxylates which can be hydrolyzed only under acidic conditions.[11,22] This reversible modification of the primary amine group to carboxylate could induce charge conversion between positive and negative in an acidic pH sensitive manner, which may reduce the cytotoxicity and minimize nonspecific cellular uptake at physiological pH conditions. According to previous studies, the hypoxic conditions due to high metabolic rate and abnormal blood vessels in tumors accumulate lactic acid and promote accelerated oxidation of CO_2, providing an acidic extracellular tumor microenvironment (pH 5.8–7.1).[23–25] This acidic pH has been used as a triggering signal for the cancer-targeted delivery of nanoparticles with drugs.[11,26–28] Conjugations of either targeting ligands or environment-sensitive moieties have been investigated for targeted delivery of nanoparticles with siRNA for diagnostic and therapeutic purpose.[3–4,8,11,28–30]

In our previous study, amine-functionalized iron oxide nanoparticles with highly stable and homogenous properties were developed for biomedical applications.[10] In the present study, three different molecules possessing distinctive functions were coated onto the amine-functionalized iron oxide nanoparticles for diagnostic and therapeutic purpose. After blocking of primary amine group in PEI using the acidic pH sensitive citraconic anhydride, the resulting amine blocked PEI was conjugated to NP for enhanced biocompatibility at pH 7.4 and recovered cytotoxic effect at acidic pH via deblocking of the amine group. Both anti-GFP siRNA and chlorotoxin (CTX) were immobilized onto NP as a therapeutic moiety and targeting ligand for glioma, respectively. The surface charge, size, stability and morphology of NP coated with amine blocked PEI, siRNA, and CTX (NP-PEIb-siRNA-CTX) were examined using dynamic light scattering and transmission electron microscopy (TEM). To investigate whether NP-PEIb-siRNA-CTX retains sufficient magnetism as a contrast agent for MRI, its magnetic property was analyzed. After conjugation of CTX, enhanced intracellular uptake of NP-PEIb-siRNA-CTX to C6 rat glioma cells was verified by the ferrozine-based assay. Cytotoxicity and gene silencing effect by NP-PEIb-siRNA-CTX was quantitatively examined at both pH 7.4 and pH 6.4 with C6 glioma cells.

2. Experimental Section

2.1. Preparation and Characterization of Primary Amine Blocked PEI

Two types of amine blocked PEIs (BPEI), the less amine group blocked PEI (PEIa) and highly amine blocked PEI (PEIb), were prepared for this study. After performing 1/10 dilution of citraconic anhydride with dimethyl sulfoxide, predetermined amount of

citraconic anhydride (0.33 mg, 0.66 mg) were reacted with branched PEI (MW25k, 1 mg) in PBS for 2 hrs at room temperature for the preparation of PEIa and PEIb resulting in citraconic anhydride/primary amine group in PEI with molar ratios of 0.42 and 0.84, respectively. To inhibit intra- and intermolecular ionic interactions, reaction was performed in the presence of high salts (0.5 M NaCl). After citraconylation of PEI, the remaining amine groups were activated with SPDP (2.3 mg) overnight at room temperature to prepare pyridyldithiol modified BPEI. After the reaction, the solution was purified using Zeba™ Spin Desalting Columns (MWCO 7k) to remove excess SPDP. The relative amounts of primary amine groups in both BPEIs and pyridyldithiol activated BPEIs were determined by the fluorescamine assay according to the manufacturer's protocol. Ten microliters of fluorescamine solution in acetone at a final concentration of 7 mg/ml were mixed with each polymer solution in PBS (100 μL) and protected from light. After incubating for 10 min at room temperature, the fluorescent intensity was measured at excitation and emission wavelengths of 390 nm and 475 nm, respectively. To examine the cleavage of the blocking group from BPEI, pyridyldithiol modified PEIb was incubated in HEPES buffer at pH 7.4, 6.4, 4.5 and 0.3 for 24 hrs. The amount of exposed amine groups at each pH condition was determined by the fluorescamine assay, as reported previously.31

To examine cell cytotoxicity of both naked PEI and modified PEI, C6 cells were seeded on 24-well plates at a density of 1×10^5 cells per well, and treated with each polymer at various concentrations (0, 1, 2, 4, 8, 16, 32, 64, 128 μg/ml) for 24 hrs in DMEM medium supplemented with 10% FBS. After incubation, cells were washed with PBS three times and treated with DMEM containing 10% Alamar Blue solution for 2 hrs, according to the manufacturer's protocol. Fluorescence intensity in each sample was measured by Spectra Max microplate reader with an excitation and emission wavelength at 470 nm and 486 nm, respectively. The relative cell viability was determined by assuming untreated cells having 100% viability.

2.2. Preparation and Characterization of Multifunctional Iron Oxide Nanoparticles

Oleic acid coated iron oxide nanoparticles with a 12-nm core diameter were synthesized via thermal decomposition of iron oleate complex and coated by PEG with terminal amine groups for the preparation of amine functionalized nanoparticles (NP-NH_2), according to previous studies.10,32 After synthesis of NP-NH_2, the concentration of Fe was analyzed by inductively coupled plasma atomic emission spectroscopy (ICP-AES). The number of amine groups per NP (~70 NH_2/NP) was determined by quantifying pyridine-2-thione using SPDP, according to the manufacturer's protocol. The NP (280 μg) in 0.1 M sodium bicarbonate buffer (pH 8.5) was mixed with Traut's reagent (245.7 μg) for the preparation of thiol modified NP (NP-SH). Excess Traut's reagent was removed using Zeba™ Spin Desalting Columns (MWCO 40k) according to the manufacturer's protocol. Pyridyldithiol activated PEIb (75 μg) was added to NP-SH at a 1:50 molar ratio of NP:PEIb and reacted for 24 hrs to prepare amine-blocked PEI coated NP (NP-PEIb). To prepare siRNA with a free thiol group (siRNA-SH), 100 μL of 1M dithiothreitol (DTT) in DW was added to 100 μL of 5′-end thiol-blocked siRNA (0.96 mM) in PBS. The final pH of the solution was adjusted to 8.0 using 5N NaOH. After an overnight reaction, the reactant was purified using Zeba™ Spin Desalting Columns (MWCO 7k). Both siRNA-SH (134.4 μg) and $SM(PEG)_2$ (4.25 μg) were added to NP-PEIb and reacted for 10 hrs for the preparation of NP-PEIb-siRNA at a 1:100 molar ratio of NP: siRNA.

Chlorotoxin (CTX, MW8000) was recombinantly synthesized in *Escherichia coli* using a method reported previously.33 Talon Resin pure CTX was further purified using size exclusion liquid chromatography, and characterized using polyacrylamide gel electrophoresis. CTX (500 μg) in PBS was reacted with Traut's reagent at a 1:1 molar ratio of Traut's reagent:CTX for 1 hr at room temperature. The pH of the reactant solution was

adjusted to 8.0 using 1N NaOH. Thiolated CTX (200 μg) and $SM(PEG)_{12}$ (12.97 μg) were added to NP-PEIb-siRNA at a 1:200 molar ratio of NP:CTX and reacted overnight. The resultant NP-PEIb-siRNA-CTX was purified using Zeba™ Spin Desalting Columns (MWCO 40k) equilibrated with PBS, and stored at 4°C. TEM samples were observed on a Phillips CM100 TEM (Philips, Eindhoven, The Netherlands) operating at 100 kV. The surface charge and hydrodynamic size of nanoparticles were analyzed using a Malvern Nano Series ZS particle size analyzer (Worcestershire, UK).

2.3. Quantification of Intracellular Iron Content

C6 cells were maintained in DMEM (Invitrogen, Carlsbad, CA) supplemented with 10% FBS (Atlanta Biologicals, Lawrenceville, GA) and 1% antibiotic-antimycotic (Invitrogen, Carlsbad, CA) at 37°C and 5% CO_2. C6 cells stably expressing GFP (GFP+ C6) were prepared by transfecting C6 cells with the pEGFP-N1 vector using Effectene transfection reagent (Qiagen, Valencia, CA) according to the manufacturer's protocol. The day before transfection, cells were plated at a density of 3×10^5 cells per well in 12-well plates. Cells were then treated with five types of iron oxide nanoparticles, NP, NP-SH, NP-PEIb, NP-PEIb-siRNA, and NP-PEIb-siRNA-CTX, at an Fe concentration of 4 μg/mL for 6 hrs at pH 7.4 and pH 6.4. After incubation, cells were washed with PBS and lysed with 400 μL of 50 mM NaOH solution. Intracellular Fe content was determined by the colorimetric ferrozine-based assay as previously described.34 Absorbance of each sample was measured at 562 nm using the Spectra Max microplate reader. The number of cells was also determined by the Coomassie Blue assay according to the manufacturer's protocol.

2.4. In vitro MRI

C6 cells (5×10^5 cells/well) were seeded on a 12-well plate 24 hrs before treatment. Cells were treated with nanoparticles in growth media (20 μg Fe/mL) at pH 6.4 and incubated for 24 hrs. After incubation, cell pellets were prepared by centrifugation at 1500 g for 5 min. Cell pellets were resuspended in 50 μL of 1% agarose. For nanoparticle samples, 25 μL of nanoparticles at various Fe concentrations (0.125, 1.25, 2.5, 5, 10 μg/mL) in PBS were mixed with 25 μL of 1% agarose. T2 relaxation measurements were performed on a 4.7-T Bruker magnet (Bruker Medical Systems, Karlsruhe, Germany) equipped with Varian Inova spectrometer (Varian, Inc., Palo Alto, CA). A 5 cm volume coil and the spin-echo imaging sequence were used to acquire T2-weight images. Images were acquired using a repetition time (TR) of 3000 ms and echo times (TE) of 13.6, 20.0, 40.0, 60.0, 90.0 and 120.0 ms. The spatial resolution parameters were: acquisition matrix of 256 × 128, field-of-view of 35 × 35 mm, section thickness of 1 mm and two averages. The T2 map was generated by NIH ImageJ (Bethesda, MD) based on the equation, $SI = A \exp(-TE/T2) + B$, where SI is the signal intensity, TE is the echo time, A is the amplitude, and B is the offset. R2 maps were generated by taking the reciprocal of T2 maps.

2.5. Cell Viability and Gene Silencing Effect

Cells were seeded on 24-well plates at a density of 1×10^5 cells per well, and treated with nanoparticles (8 μ*g* Fe/ml) for 48 hrs in DMEM supplemented with 10% FBS at pH 7.4 and pH 6.4. After incubation, cell viability was examined by the Alamar blue assay. To quantify the degree of GFP gene silencing, the cells were transfected with various amounts of nanoparticles (0, 0.5, 1, 2, 4, 8 μg Fe) for 24 hrs in the presence of serum at pH 7.4 and pH 6.4 and incubated for an additional 24 hrs after changing medium with DMEM with 10% FBS. After transfection, cells were washed with PBS three times and treated with a cell lysis solution (1% Triton X-100 in PBS). GFP protein expression was measured at an excitation and an emission wavelength of 488 and 520 nm, respectively. The extent of GFP fluorescence was normalized by the total viable cells, which was determined by the Alamar

Blue assay. Relative GFP expression levels were then calculated based on the GFP expression percent of non-transfected C6 cells used as a 100% control.

3. Results

3.1. Preparation and Characterization of Amine Group Blocked PEI

The scheme for synthesis of primary amine blocked PEI (25k) is shown in Figure 1a. The primary amine group of PEI was blocked by citraconic anhydride, an acid pH specific amine blocker. After citraconylation reaction, the primary amine groups are replaced with carboxyl groups, which changes the total cationic charge in PEI. The remaining amine groups in PEI are then activated with SPDP to produce 2-pyridyl disulfide activated PEI for the following conjugation onto iron oxide nanoparticles (NPs). After each reaction, the amount of remaining amine groups was quantitatively examined using the fluorescamine assay. As shown in Figure 2a, two different types of amine blocked PEI, less amine blocked PEI (PEIa) and highly amine blocked PEI (PEIb), were prepared by adding different amounts of citraconic anhydride. Molar fractions of primary, secondary, and tertiary amine groups in PEI were 0.307, 0.395, and 0.297, respectively. Based on this, the molar ratios of citraconic anhydride per primary amine group in PEI for the preparation of PEIa and PEIb were 0.42:1 and 0.84:1, respectively. After citraconylation, 64.9 ± 3.8 and 28.9 ± 12.4% of primary amine groups in PEIa and PEIb remained, respectively. Approximately 10% of amine groups were also activated by SPDP in both PEIs.

To examine whether blocking of primary amine groups in PEI could reduce nonspecific cytotoxicity, cell viability was examined after treated with naked PEI, PEIa, and PEIb (Fig. 2b). Both naked PEI and PEIa treated cells showed severe cell toxicity with increasing PEI concentrations, while the PEIb group demonstrated negligible cytotoxic effect. To confirm the removal of blocking groups in PEI in an acidic pH-dependent manner, the amount of exposed amine in PEIb was quantitatively examined after incubating PEIb at different pHs (Fig. 2c). The extent of exposed primary amine groups in PEIb at pH 7.4, 6.4, and 4.5 were 1.9 ± 2.1, 8.8 ± 2.0, and 39.5 ± 6.4 %, respectively, demonstrating that the deblocking of the primary amine groups occurs only in acidic pH conditions.

To confirm that the deblocking of primary amine groups in PEIb in acidic conditions could recover cell toxicity comparable to naked PEI, cytotoxicities by naked PEI and PEIb before and after acid treatment were examined (Fig. 2d). The PEIb treated with acid treatment exhibited significantly increased cytotoxicity compared to PEIb at pH 7.4, suggesting that the cytotoxicity of this polymer can be elicited by an acidic environment. However, the extent of cytotoxic effect by PEIb treated with acid was a little reduced than that by naked PEI, which is probably due to the noncleavable blocking of primary amine groups in PEI by SPDP.

3.2. Preparation and Characterization of Multifunctional Iron Oxide Nanovectors

In our previous study, NPs were modified with amine functionalized PEG to improve stability and reduce nonspecific cellular uptake for MR imaging.10 Here, the pH-sensitive PEIb developed above was used for the surface modification of the NP-NH_2 (Fig. 1a). Primary amine groups on NP were reacted with Traut's reagent to produce free thiol modified NP (NP-SH). The pyridyldithiol activated PEIb prepared by SPDP reaction was added to thiol modified NP, which resulted in blocked PEI coated NP (NP-PEIb). The chemical scheme used to assemble siRNA and chlorotoxin (CTX) on the NP surface are shown in Figure 1b. The thiol-modified siRNA at the sense 5′ end was conjugated to the free amine groups available on PEIb and NP using $SM(PEG)_2$ as a crosslinker. For enhanced intracellular delivery of the nanovector for glioma cells, CTX was also immobilized to the

NP-PEIb-siRNA conjugate. Chlorotoxin, a 36 amino-acid peptide derived from scorpion *Leiurus quinquestriatus*, is a well-known targeting ligand for malignant glioma, medulloblastoma, and prostate cancers.[19,30,35–36] Thiol-modified CTX by Traut's reagent was covalently attached to NP-PEIb-siRNA conjugate via $SM(PEG)_{12}$ crosslinker for the preparation of NP-PEIb-siRNA-CTX.

To quantify and optimize the extent of conjugated siRNA to NP, the NP-PEIb-siRNA-CTX nanovector was assessed by agarose gel electrophoresis (Fig. 3a). The siRNA conjugated to NP-PEIb-siRNA-CTX showed a retarded and smear band on agarose gel because of the increased size of the resulting nanovector compared to naked siRNA as well as varying numbers of attached siRNA on individual nanoparticles. The relative amount of siRNA conjugated to nanoparticles for 1 μg and 2 μg siRNA were 37.6 ± 7.4 % and 28.9 ± 7.8 % of total feed siRNA, respectively, as determined by densitometry using ImageJ software (National Institute of Health, USA; http://rsb.info.nih.gov/ij/). To confirm that this retarded migration of NP-PEIb-siRNA-CTX is not attributed to ionic interaction between siRNA and PEIb, a physical mixture of siRNA and NP-PEIb at the same PEIb/siRNA weight ratio as that of the NP-PEIb-siRNA-CTX conjugates was also examined by gel electrophoresis. As shown in Figure 3b, NP-PEIb could not form ionic complexes with siRNA while naked PEI/siRNA complexes showed no migration due to ionic interactions, suggesting that the retarded migration of siRNA in NP-PEIb-siRNA-CTX nanovector is due to the covalent linkage of siRNA to NP rather than the electrostatic interaction between PEIb and siRNA .

The average surface charge and hydrodynamic size of the resulting five different types of nanoparticles were determined by dynamic light scattering (DLS). (Fig. 4a–b). Conjugation of PEIb onto NP-SH increased surface charge from −12.4 ± 2.8 mV to −2.6 ± 0.7 mV at pH 7.4 due to both remnant primary amine groups and intact secondary and tertiary amine groups. However, after siRNA conjugation, the surface charge of nanoparticles decreased to −14.6 ± 2.2 mV because of the highly negatively charged siRNA. The surface charges of NP-PEIb-siRNA-CTX at pH 7.4 and pH 6.4 were −14.1 ± 1.9 mV and −5.2 ± 1.3 mV, respectively. Considering that there were ~174 primary amine group per every PEI, a 10% recovery of amine groups at pH 6.4 could substantially increase the surface charge. The hydrodynamic sizes of each type of nanoparticles at pH 7.4 and pH 6.4 are shown in Figure 4b. While there were significant changes in surface charge after conjugation of PEIb and siRNA, little differences in particle size were observed among NP, NP-SH, NP-PEIb, and NP-PEIb-siRNA. Despite the significant differences in surface charge at different pHs, the size of each nanoparticle was pretty constant, which might be due to sufficient PEG shielding on nanovector. However, the diameter of NP-PEIb-siRNA-CTX at pH 6.4 (107.4 ± 6.7 nm) was significantly larger than that at pH 7.4 (63.7 ± 8.4 nm) (Fig. 4b). Considering that the pore size of 1% agarose gel was more than 350 nm,[37] the nanoparticles with a size below 70 nm could easily pass through the agarose gel as shown in Figure 3a.

For biomedical applications, long-term stability of nanoparticles is an important factor considered during design of nanoparticles. To examine the stability of NP-PEIb-siRNA-CTX, size distributions of nanoparticles both as prepared and after 28 days in PBS solution were analyzed. As shown in Figure 4c, negligible changes in particle size were observed between the two, suggesting the high stability of NP-PEIb-siRNA-CTX. The core particle size and morphology of NP-PEIb-siRNA-CTX was examined with TEM (Fig. 4d). NP-PEIb-siRNA-CTX was spherical and well-dispersed, with a core size of ~12 nm, indicating that there was no aggregation or inter-crosslinking between particles during conjugation reaction.

3.3. Magnetic Property and Intracellular Uptake of NP-PEIb-siRNA-CTX

The iron oxide core of this NP system has been previously shown to possess superior superparamagnetic properties essential for use as a contrast agent for MR imaging.10 To evaluate whether NP-PEIb-siRNA-CTX would retain sufficient magnetism detectable by MRI, the relaxation of NP-PEIb-siRNA-CTX at various concentrations of Fe was measured. The transverse relaxivity (slope of R2) of NP-PEIb-siRNA-CTX was 673 mM^{-1} S^{-1} (Fig. 5a), significantly higher than that of Feridex (~230 mM^{-1} S^{-1}), a commercial T2 contrast agent, making NP-PEIb-siRNA-CTX potentially a very effective T2 contrast agent for MRI. Figure 5b shows that relaxation (R2) changes of agarose phantom casts with NP-PEIb-siRNA-CTX with increasing Fe concentration, could be readily detected by MRI in a dose dependent manner.

To confirm that conjugation of CTX could enhance intracellular uptake of nanoparticles, the amount of intracellular Fe per cell was quantified using a ferrozine-based assay after treating C6 cells with five different nanoparticles at an Fe concentration of 4 μg/mL for 6 hrs. As shown in Figure 5c, NP-PEIb-siRNA-CTX exhibited 2–4 fold higher Fe uptake than NP-SH, NP-PEIb, and NP-PEIb-siRNA at pH 6.4. The enhanced intracellular uptake of NP-PEIb-siRNA-CTX over that of NP-PEIb-siRNA despite the similar surface charge exhibited by the two nanovectors suggests that the immobilization of CTX facilitated the cellular internalization of the nanovector. This enhanced cellular uptake was also visualized by T2-weighted MR images of cells incubated with different nanoparticles (Fig. 5d). Cells incubated with NP-PEIb-siRNA-CTX generated the darkest image compared to those treated with NP-NH_2, NP-SH, or NP-PEIb.

3.4. Cell Toxicity and Gene Silencing Effect by NP-PEIb-siRNA-CTX

Figure 6a shows the elicited cytotoxic effect in C6 cells treated with four different types of nanoparticles at both pH 7.4 and pH 6.2. While no significant cytotoxicity was elicited by any of these nanoparticles at pH 7.4, nanoparticles coated with PEIb (i.e., NP-PEIb-siRNA and NP-PEIb-siRNA-CTX) exhibited greatly enhanced cytotoxic effect at pH 6.2, indicating that nanoparticles coated with amine group-blocked PEI induced pH-specific cell-killing for cancer cells. NP-PEIb-siRNA elicited significant cytotoxicity at pH 6.2 but not at all at pH 7.4. The viabilities of cells treated with NP-PEIb-siRNA-CTX at pH 7.4 and pH 6.2 were 77.2 ± 3.7% and 19.1 ± 0.8%, respectively. There was no cytotoxic effect on C6 cells by acidic pH itself down to pH 5.4 (data not shown). This is likely due to cancer cells having their own mechanism of survival in acidic extracellular conditions.24,38

Gene silencing effects by NP-PEIb-siRNA-CTX were evaluated at both pH 7.4 and pH 6.2 in the presence of 10% serum (Fig. 6b). The extent of GFP gene expression by cells treated with NP-PEIb-siRNA-CTX at pH 6.2 was significantly decreased with increasing amount of NP-PEIb-siRNA-CTX, while little change in GFP gene expression was observed in cells receiving the same treatments at pH 7.4. As shown in Figure 4a, the negative surface charge on NP-PEIb-siRNA-CTX at pH 7.4 is nearly 3 times greater than that at pH 6.2. This highly negatively charged nanovector at pH 7.4 could hinder its cellular internalization, resulting in substantially-reduced gene silencing. The relative percentages of GFP gene expression after transfecting C6 cells with 8 μg of NP-PEIb-siRNA-CTX at pH 7.4 and pH 6.2 were 93.8 ± 12.9% and 50.8 ± 8.8%, respectively. However, commercial naked PEI/siRNA complexes at the same weight ratio (the ratio of nitrogen in PEI/phosphate in siRNA = 1.4) as NP-PEIb-siRNA-CTX did not showed any gene silencing effect in 10% serum medium (data not shown). Previous study also indicated that naked PEI/siRNA complexes showed negligible gene silencing effect up to nitrogen in PEI/phosphate in siRNA ratio of 8 in the presence of 10% serum.39 NP-siRNA without PEI coating showed negligible gene silencing or

cytotoxic effect, which is probably due to the limited cellular internalization and escape from endosomes after intracellular uptake (data not shown).

4. Discussion

To reduce nonspecific cytotoxicity and haemolysis by PEI while maintaining superior gene transfection efficiency, various noncleavable chemical modification of primary amine groups such as acylation and alkylation in PEI have been reported.[13,17,20–21] In this study, the primary amines of PEI were blocked by citraconic anhydride, which showed excellent biocompatibility. The resultant PEIb exhibited no cytotoxic effect up to a polymer concentration of 120 μg/mL, compared to acetylated PEI which showed severe cytotoxicity at a polymer concentration of 40 μg/mL.[21] Moreover, the blocking of primary amine groups using citraconic anhydride is reversible in acidic pH conditions, enabling triggered cytotoxicity only at acidic pH of the common tumor microenvironment.

The nanoparticles conjugated with blocked PEI showed significant increase in surface charge at pH 6.4 compared to that at pH 7.4, while there were negligible differences in surface charge of NP-NH_2 and NP-SH at these two different pH conditions. This might be attributed to both the removal of blocking groups in primary amine groups and protonation of secondary/tertiary amines in PEI. This increase in surface charge in acidic pH resulted in enhanced intracellular uptake of nanovectors in the tumor microenvironment. The presence of CTX on NP-PEIb-siRNA-CTX further enhanced the nanovector uptake by target cells.

Nanoparticles designed for *in vivo* applications are preferred to have a diameter less than 100 nm to facilitate their navigation through the body, retain a long blood circulation time, and enhance permeability through blood vessels in the tumor microenvironment.[40–41] The size of the resulting nanovector (NP-PEIb-siRNA-CTX) at the physiological condition was ~63 nm, suggesting that these nanovectors could be accumulated in tumor tissues via the enhanced permeability and retention effect. The increased hydrodynamic size of NP-PEIb-siRNA-CTX at pH 6.2 could be attributed to stretching out of CTX conjugated via dodecaethyleneglycol as a spacer. CTX is a cationic peptide with three lysines and two arginines per every 36 amino acids. The removal of blocking groups at acidic pH could result in increased surface charge, which may induce more favorable exposure of cationic CTX outward from NP-PEIb-siRNA-CTX via electrostatic charge repulsion.

In the design of this nanovector (Fig. 1c), it was hypothesized that the NP-PEIb-siRNA-CTX is highly negatively charged at the physiological pH but increases its surface charge in the acidic tumor extracellular microenvironment via both deblocking of some primary amine groups and protonation of remnant amine groups in PEI. Both the increased surface charge at acidic pH and the presence of targeting ligand CTX on the nanovector would enhance cellular uptake of the nanovector. Once the nanovector is endocytosed, the secondary and tertiary amine groups in PEI on the nanovector would facilitate its endosomal escape via the proton sponge effect.[42] Upon escape from the endosome, the siRNA is released from the nanovector by cleavage of the disulfide linkage in the reductive cytosolic condition and provides therapeutic effect through gene silencing. As expected, NP-PEIb-siRNA-CTX exhibited significantly increased gene silencing effect at pH 6.2, compared to that at pH 7.4 (Figure 6b). It should also be noted that PEI was conjugated to NP via cleavable disulfide linkage in this study, which could be dissociated in the reductive cytosol.[1] The PEI with recovered primary amine groups could be released from NP in the cytosol, which might facilitate destabilization of mitochondrial membranes and activation of apoptotic signals for cytotoxic effect. There was no cytotoxic effect on C6 cells by acidic pH itself up to pH 5.4 (data not shown). This is likely due to cancer cells having their own mechanism of survival in acidic extracellular conditions.[24,38] At pH 6.4, NP-PEIb-siRNA-CTX elicited the most

significant cytotoxicity, as compared to other nanoparticles, as a result of both the deblocking of the primary amine groups on PEIb and enhanced cellular internalization of the nanovector by CTX. NP-PEIb-siRNA-CTX elicited a slightly higher cytotoxic effect (~20%) than NP-PEIb-siRNA at pH 7.4, which might be attributed to the partial deblocking of the primary amine groups of PEIb in the endosomal/lysosomal acidic environment[22,43] after the cellular uptake of NP-PEIb-siRNA-CTX. This can be attributed to the enhanced intracellular uptake of NP-PEIb-siRNA-CTX due to the presence of CTX as compared to NP-PEIb-siRNA.

In this study, superparamagnetic iron oxide nanoparticles have been successfully modified with three different functional molecules for enhanced cytotoxicity and gene silencing in cancer cells. NP-PEIb-siRNA-CTX retained sufficient magnetism for MR imaging. CTX conjugation to nanoparticles induced significantly enhanced intracellular uptake of nanovectors by C6 glioma cells. Moreover, cytotoxicity and gene silencing effect by NP-PEIb-siRNA-CTX were only observed in acidic pH conditions. These results suggest that this nanovector system, with dual targeting specificity and dual therapeutic effect, could be safely applied as a potential therapeutic imaging agent for the targeted treatment of glioma as well as other cancers.

Acknowledgments

This work is supported in part by NIH grants (R01CA134213 and R01EB006043). O. Veiseh and F. Kievit acknowledge the support through an NCI training grant (T32CA138312). C. Fang acknowledges the support through an NCI/NSF IGERT fellowship. J. Park acknowledges the support through the ASAF fellowship. We acknowledge the use of resources at the Diagnostic Imaging Sciences Center, Animal Bioimaging Center, Center for Nanotechnology, Department of Immunology, and Keck Microscopy Imaging Facility at the University of Washington.

References

1. Mok H, Lee SH, Park JW, Park TG. Multimeric small interfering ribonucleic acid for highly efficient sequence-specific gene silencing. Nat Mater. 2010; 9(3):272–278. [PubMed: 20098433]
2. Extance A. Targeting RNA: an emerging hope for treating muscular dystrophy. Nat Rev Drug Discov. 2009; 8(12):917–918. [PubMed: 19949390]
3. Derfus AM, Chen AA, Min DH, Ruoslahti E, Bhatia SN. Targeted quantum dot conjugates for siRNA delivery. Bioconjug Chem. 2007; 18(5):1391–1396. [PubMed: 17630789]
4. Lee JH, Lee K, Moon SH, Lee Y, Park TG, Cheon J. All-in-one target-cell-specific magnetic nanoparticles for simultaneous molecular imaging and siRNA delivery. Angew Chem Int Ed Engl. 2009; 48(23):4174–4179. [PubMed: 19408274]
5. Ghosh PS, Kim CK, Han G, Forbes NS, Rotello VM. Efficient gene delivery vectors by tuning the surface charge density of amino acid-functionalized gold nanoparticles. ACS Nano. 2008; 2(11): 2213–2218. [PubMed: 19206385]
6. Lee JS, Green JJ, Love KT, Sunshine J, Langer R, Anderson DG. Gold, poly(beta-amino ester) nanoparticles for small interfering RNA delivery. Nano Lett. 2009; 9(6):2402–2406. [PubMed: 19422265]
7. Shubayev VI, Pisanic TR 2nd, Jin S. Magnetic nanoparticles for theragnostics. Adv Drug Deliv Rev. 2009; 61(6):467–477. [PubMed: 19389434]
8. Kievit FM, Veiseh O, Bhattarai N, Fang C, Gunn JW, Lee D, Ellenbogen RG, Olson JM, Zhang M. PEI-PEG-Chitosan Copolymer Coated Iron Oxide Nanoparticles for Safe Gene Delivery: synthesis, complexation, and transfection. Adv Funct Mater. 2009; 19(14):2244–2251. [PubMed: 20160995]
9. Hussain SM, Hess KL, Gearhart JM, Geiss KT, Schlager JJ. In vitro toxicity of nanoparticles in BRL 3A rat liver cells. Toxicol In Vitro. 2005; 19(7):975–983. [PubMed: 16125895]
10. Fang C, Bhattarai N, Sun C, Zhang M. Functionalized nanoparticles with long-term stability in biological media. Small. 2009; 5(14):1637–1641. [PubMed: 19334014]

11. Mok H, Park JW, Park TG. Enhanced intracellular delivery of quantum dot and adenovirus nanoparticles triggered by acidic pH via surface charge reversal. Bioconjug Chem. 2008; 19(4): 797–801. [PubMed: 18363345]
12. Xiang JJ, Tang JQ, Zhu SG, Nie XM, Lu HB, Shen SR, Li XL, Tang K, Zhou M, Li GY. IONP-PLL: a novel non-viral vector for efficient gene delivery. J Gene Med. 2003; 5(9):803–817. [PubMed: 12950071]
13. Thomas M, Klibanov AM. Enhancing polyethylenimine's delivery of plasmid DNA into mammalian cells. Proc Natl Acad Sci U S A. 2002; 99(23):14640–14645. [PubMed: 12403826]
14. Park TG, Jeong JH, Kim SW. Current status of polymeric gene delivery systems. Adv Drug Deliv Rev. 2006; 58(4):467–486. [PubMed: 16781003]
15. Song WJ, Du JZ, Sun TM, Zhang PZ, Wang J. Gold nanoparticles capped with polyethyleneimine for enhanced siRNA delivery. Small. 2010; 6(2):239–246. [PubMed: 19924738]
16. Hunter AC. Molecular hurdles in polyfectin design and mechanistic background to polycation induced cytotoxicity. Adv Drug Deliv Rev. 2006; 58(14):1523–1531. [PubMed: 17079050]
17. Fischer D, Li Y, Ahlemeyer B, Krieglstein J, Kissel T. In vitro cytotoxicity testing of polycations: influence of polymer structure on cell viability and hemolysis. Biomaterials. 2003; 24(7):1121–1131. [PubMed: 12527253]
18. Hoon Jeong J, Christensen LV, Yockman JW, Zhong Z, Engbersen JF, Jong Kim W, Feijen J, Wan Kim S. Reducible poly(amido ethylenimine) directed to enhance RNA interference. Biomaterials. 2007; 28(10):1912–1917. [PubMed: 17218006]
19. Veiseh O, Kievit FM, Gunn JW, Ratner BD, Zhang M. A ligand-mediated nanovector for targeted gene delivery and transfection in cancer cells. Biomaterials. 2009; 30(4):649–657. [PubMed: 18990439]
20. Aravindan L, Bicknell KA, Brooks G, Khutoryanskiy VV, Williams AC. Effect of acyl chain length on transfection efficiency and toxicity of polyethylenimine. Int J Pharm. 2009; 378(1–2): 201–210. [PubMed: 19501146]
21. Gabrielson NP, Pack DW. Acetylation of polyethylenimine enhances gene delivery via weakened polymer/DNA interactions. Biomacromolecules. 2006; 7(8):2427–2435. [PubMed: 16903692]
22. Lee Y, Fukushima S, Bae Y, Hiki S, Ishii T, Kataoka K. A protein nanocarrier from charge-conversion polymer in response to endosomal pH. J Am Chem Soc. 2007; 129(17):5362–5363. [PubMed: 17408272]
23. Vaupel PW, Frinak S, Bicher HI. Heterogeneous oxygen partial pressure and pH distribution in C3H mouse mammary adenocarcinoma. Cancer Res. 1981; 41(5):2008–2013. [PubMed: 7214369]
24. Mashima T, Sato S, Sugimoto Y, Tsuruo T, Seimiya H. Promotion of glioma cell survival by acyl-CoA synthetase 5 under extracellular acidosis conditions. Oncogene. 2009; 28(1):9–19. [PubMed: 18806831]
25. Swietach P, Vaughan-Jones RD, Harris AL. Regulation of tumor pH and the role of carbonic anhydrase 9. Cancer Metastasis Rev. 2007; 26(2):299–310. [PubMed: 17415526]
26. Min KH, Kim JH, Bae SM, Shin H, Kim MS, Park S, Lee H, Park RW, Kim IS, Kim K, Kwon IC, Jeong SY, Lee DS. Tumoral acidic pH-responsive MPEG-poly(beta-amino ester) polymeric micelles for cancer targeting therapy. J Control Release. 2010; 144(2):259–266. [PubMed: 20188131]
27. Sethuraman VA, Na K, Bae YH. pH-responsive sulfonamide/PEI system for tumor specific gene delivery: an in vitro study. Biomacromolecules. 2006; 7(1):64–70. [PubMed: 16398499]
28. Lee ES, Gao Z, Bae YH. Recent progress in tumor pH targeting nanotechnology. J Control Release. 2008; 132(3):164–170. [PubMed: 18571265]
29. Lai JJ, Hoffman JM, Ebara M, Hoffman AS, Estournes C, Wattiaux A, Stayton PS. Dual magnetic-/temperature-responsive nanoparticles for microfluidic separations and assays. Langmuir. 2007; 23(13):7385–7391. [PubMed: 17503854]
30. Veiseh M, Gabikian P, Bahrami SB, Veiseh O, Zhang M, Hackman RC, Ravanpay AC, Stroud MR, Kusuma Y, Hansen SJ, Kwok D, Munoz NM, Sze RW, Grady WM, Greenberg NM, Ellenbogen RG, Olson JM. Tumor paint: a chlorotoxin:Cy5.5 bioconjugate for intraoperative visualization of cancer foci. Cancer Res. 2007; 67(14):6882–6888. [PubMed: 17638899]

31. Oh IK, Mok H, Park TG. Folate immobilized and PEGylated adenovirus for retargeting to tumor cells. Bioconjug Chem. 2006; 17(3):721–727. [PubMed: 16704210]
32. Park J, An K, Hwang Y, Park JG, Noh HJ, Kim JY, Park JH, Hwang NM, Hyeon T. Ultra-large-scale syntheses of monodisperse nanocrystals. Nat Mater. 2004; 3(12):891–895. [PubMed: 15568032]
33. Deshane J, Garner CC, Sontheimer H. Chlorotoxin inhibits glioma cell invasion via matrix metalloproteinase-2. J Biol Chem. 2003; 278(6):4135–4144. [PubMed: 12454020]
34. Riemer J, Hoepken HH, Czerwinska H, Robinson SR, Dringen R. Colorimetric ferrozine-based assay for the quantitation of iron in cultured cells. Anal Biochem. 2004; 331(2):370–375. [PubMed: 15265744]
35. Veiseh O, Sun C, Gunn J, Kohler N, Gabikian P, Lee D, Bhattarai N, Ellenbogen R, Sze R, Hallahan A, Olson J, Zhang M. Optical and MRI multifunctional nanoprobe for targeting gliomas. Nano Lett. 2005; 5(6):1003–1008. [PubMed: 15943433]
36. Shen S, Khazaeli MB, Gillespie GY, Alvarez VL. Radiation dosimetry of 131I-chlorotoxin for targeted radiotherapy in glioma-bearing mice. J Neurooncol. 2005; 71(2):113–119. [PubMed: 15690125]
37. Pernodet N, Maaloum M, Tinland B. Pore size of agarose gels by atomic force microscopy. Electrophoresis. 1997; 18(1):55–58. [PubMed: 9059821]
38. Chiche J, Ilc K, Laferriere J, Trottier E, Dayan F, Mazure NM, Brahimi-Horn MC, Pouyssegur J. Hypoxia-inducible carbonic anhydrase IX and XII promote tumor cell growth by counteracting acidosis through the regulation of the intracellular pH. Cancer Res. 2009; 69(1):358–368. [PubMed: 19118021]
39. Mok H, Park TG. Self-crosslinked and reducible fusogenic peptides for intracellular delivery of siRNA. Biopolymers. 2008; 89(10):881–888. [PubMed: 18521895]
40. Gupta AK, Gupta M. Synthesis and surface engineering of iron oxide nanoparticles for biomedical applications. Biomaterials. 2005; 26(18):3995–4021. [PubMed: 15626447]
41. Nie S, Xing Y, Kim GJ, Simons JW. Nanotechnology applications in cancer. Annu Rev Biomed Eng. 2007; 9:257–288. [PubMed: 17439359]
42. Yezhelyev MV, Qi L, O'Regan RM, Nie S, Gao X. Proton-sponge coated quantum dots for siRNA delivery and intracellular imaging. J Am Chem Soc. 2008; 130(28):9006–9012. [PubMed: 18570415]
43. You JO, Auguste DT. Nanocarrier cross-linking density and pH sensitivity regulate intracellular gene transfer. Nano Lett. 2009; 9(12):4467–4473. [PubMed: 19842673]

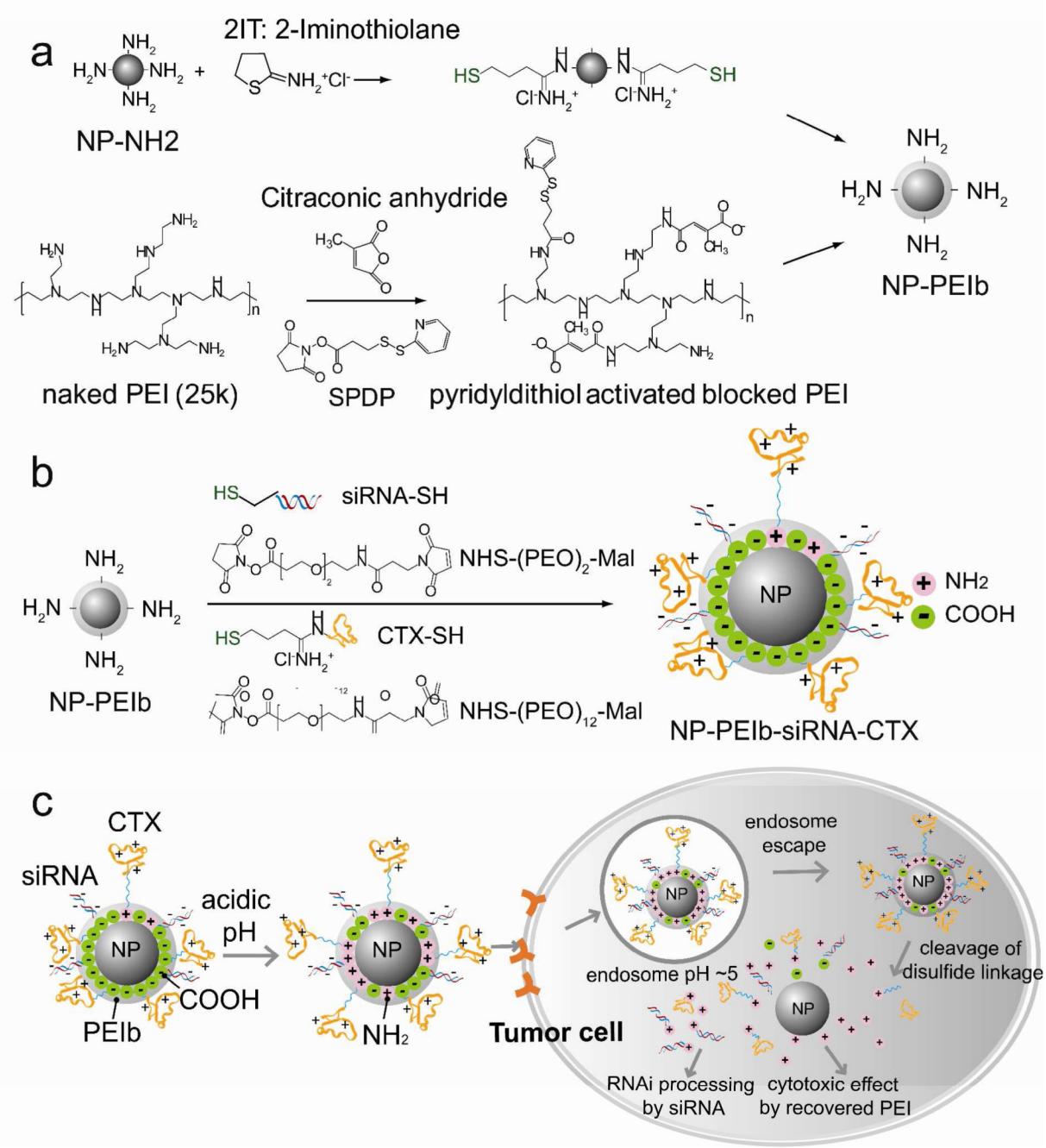

Figure 1.

Chemical schemes for development of the multifunctional nanovector and illustration of extracellular and intracellular trafficking of the nanovector. Schems for the preparation of (a) the amine blocked PEI and (b) multifunctional NP-PEIb-siRNA-CTX nanovector. (c) Schematic diagram illustrating the intracellular uptake, extracellular trafficking and processing of NP-PEIb-siRNA-CTX in tumor cells.

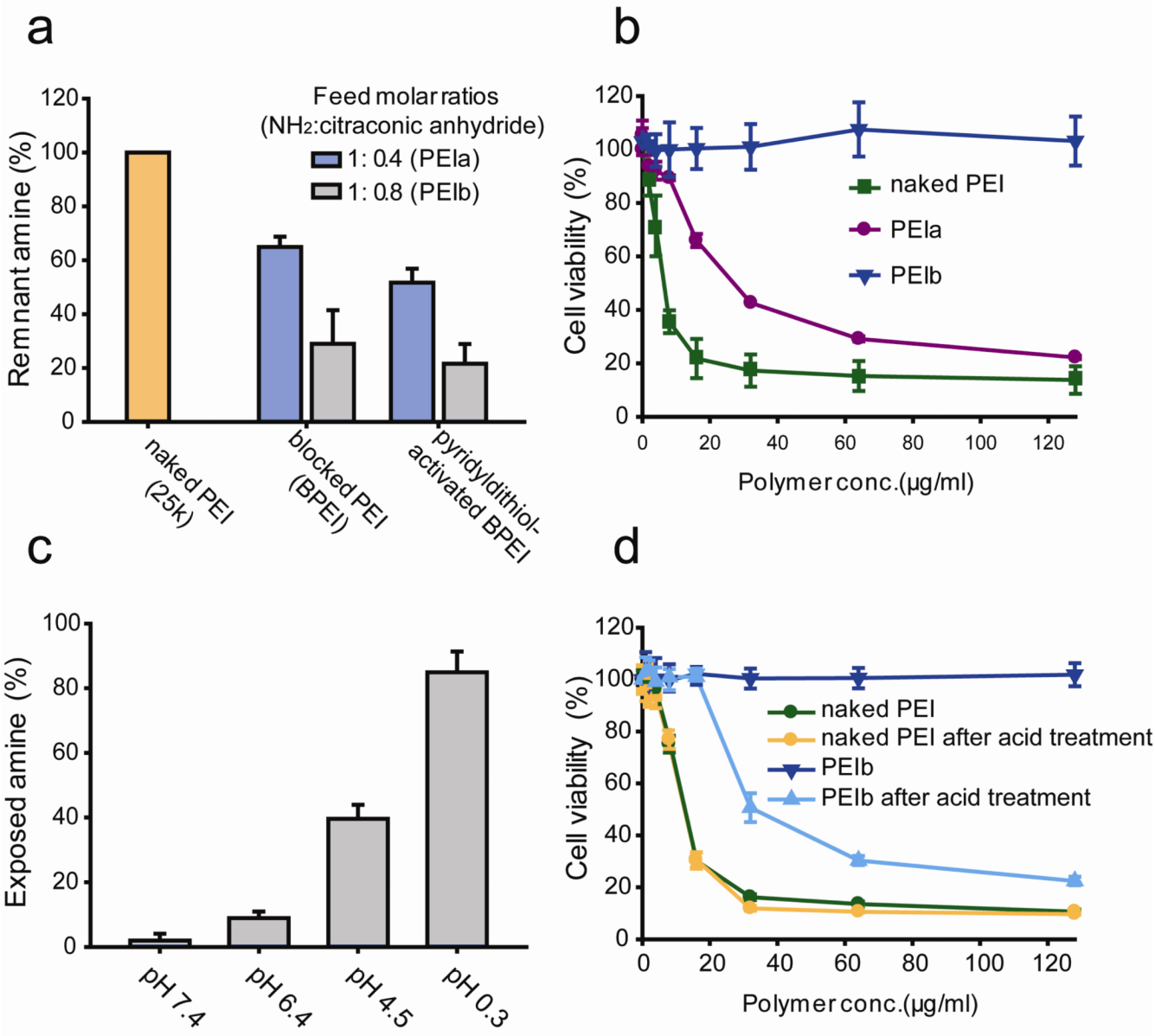

Figure 2.

Characterization of the primary amine-blocked and pyridyldithiol-activated PEI. (a) Relative amount of primary amine groups after amine blocking reaction by citraconic anhydride and pyridyldithiol reaction by SPDP using two types of PEI (PEIa and PEIb), respectively. PEIa: less amine blocked PEI, and PEIb: highly amine blocked PEI. (b) Cytotoxicities of PEIa and PEIb in C6 rat glioma cells, where the naked PEI is presented as a control. (c) Relative amount of exposed primary amine groups in PEIb after incubation for 24 hrs at various pH conditions. (d) Cytotoxicities on C6 cells by primary amine recovered PEIb at pH 0.3, where the naked PEI is presented as a reference.

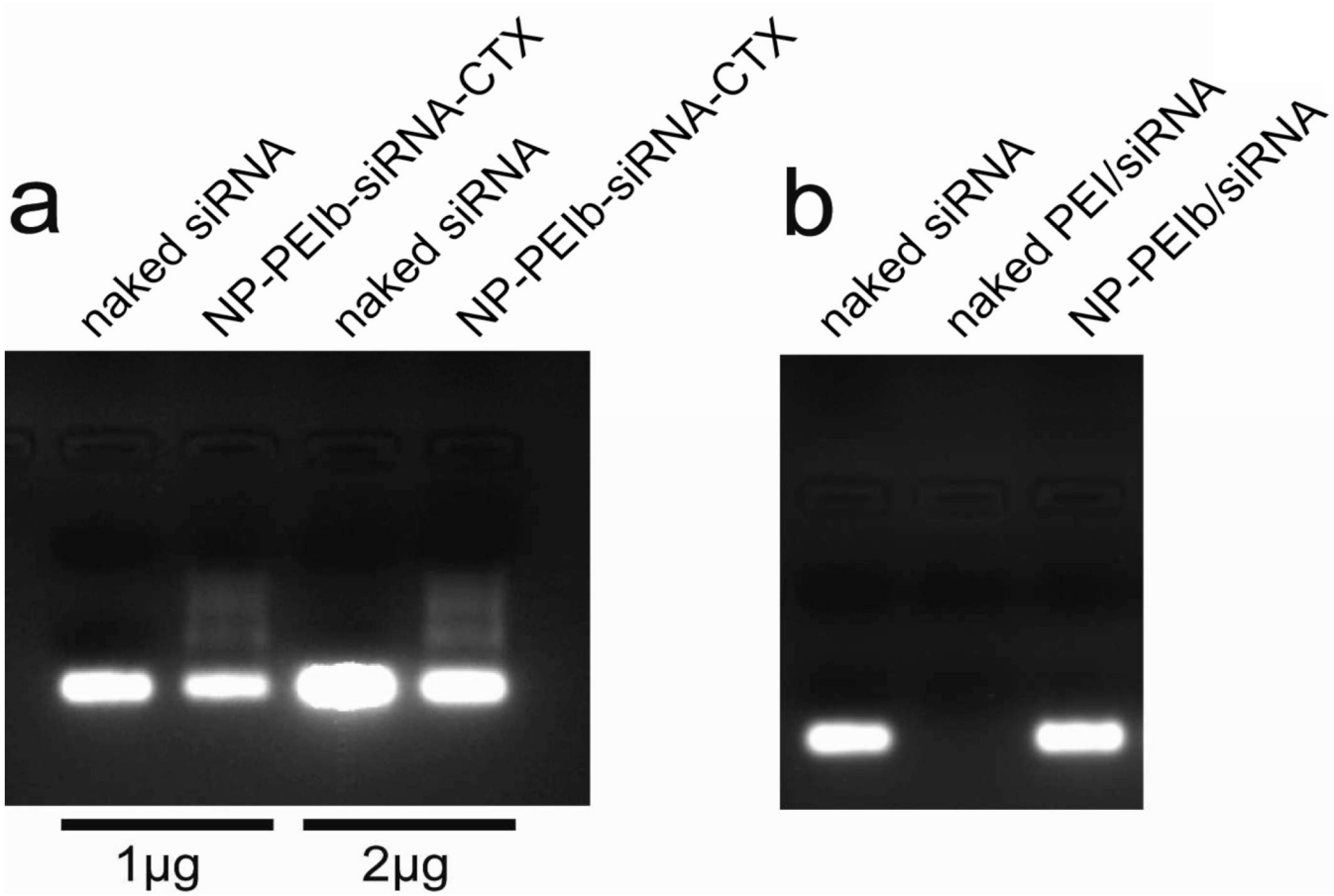

Figure 3.

Gel electrophoresis to confirm the amount of siRNA on NP and covalent conjugation of siRNA to nanovector. (a) Agarose gel electrophoresis of NP-PEIb-siRNA-CTX after conjugation of different amounts of siRNA on the nanovector, where the naked siRNA serves as a control. (b) Gel retardation assay for siRNA physically mixed with naked PEI or NP-PEIb at a PEI/siRNA weight ratio of 0.18.

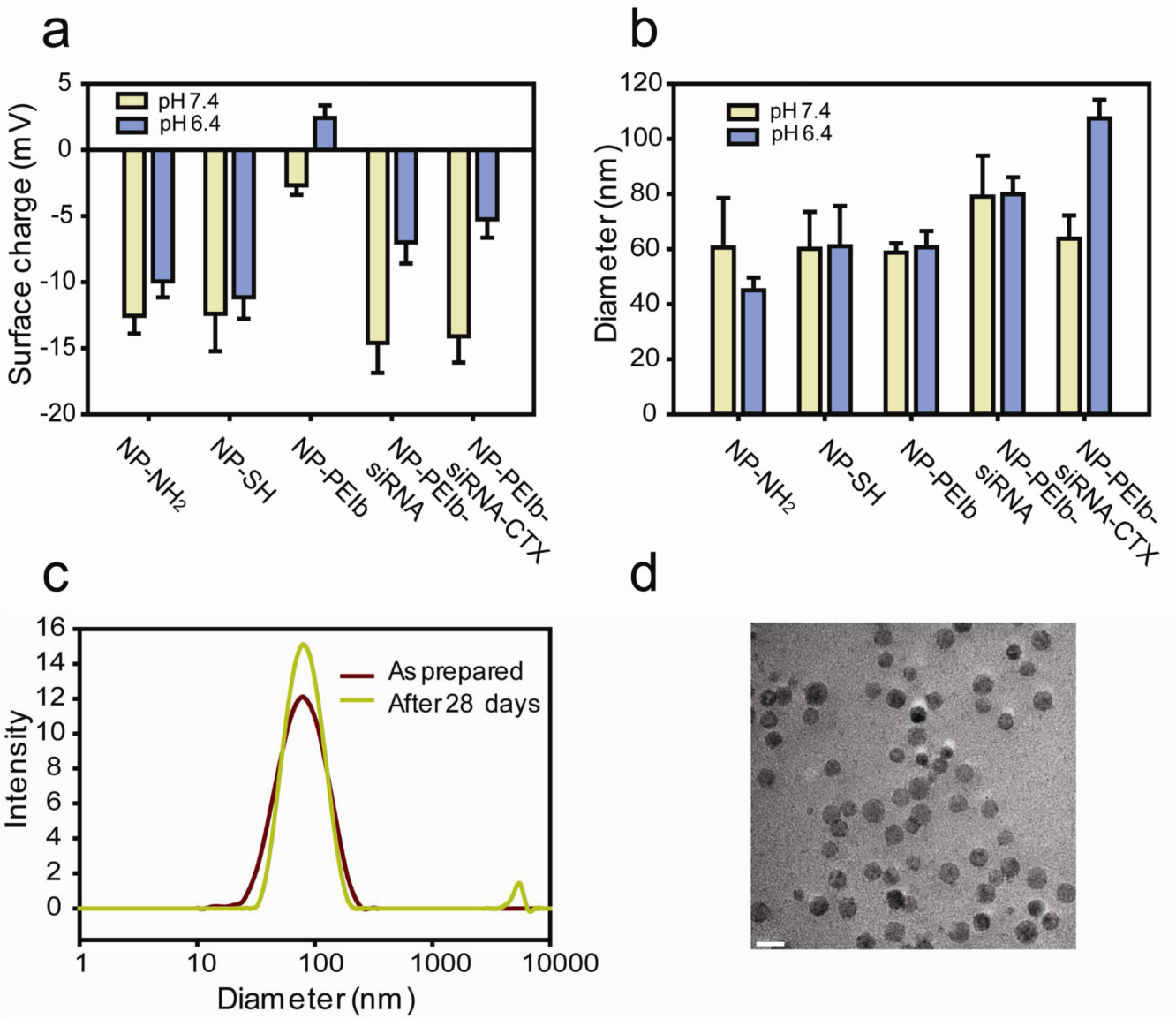

Figure 4.

Physical properties of various iron oxide nanoparticles. (a) Surface charge and (b) hydrodynamic size of different nanoparticles at pH 7.4 and pH 6.4. (c) Stability of NP-PEIb-siRNA-CTX in PBS, assessed in terms of hydrodynamic size profile. (d) TEM image of NP-PEIb-siRNA-CTX (scale bar = 20 nm).

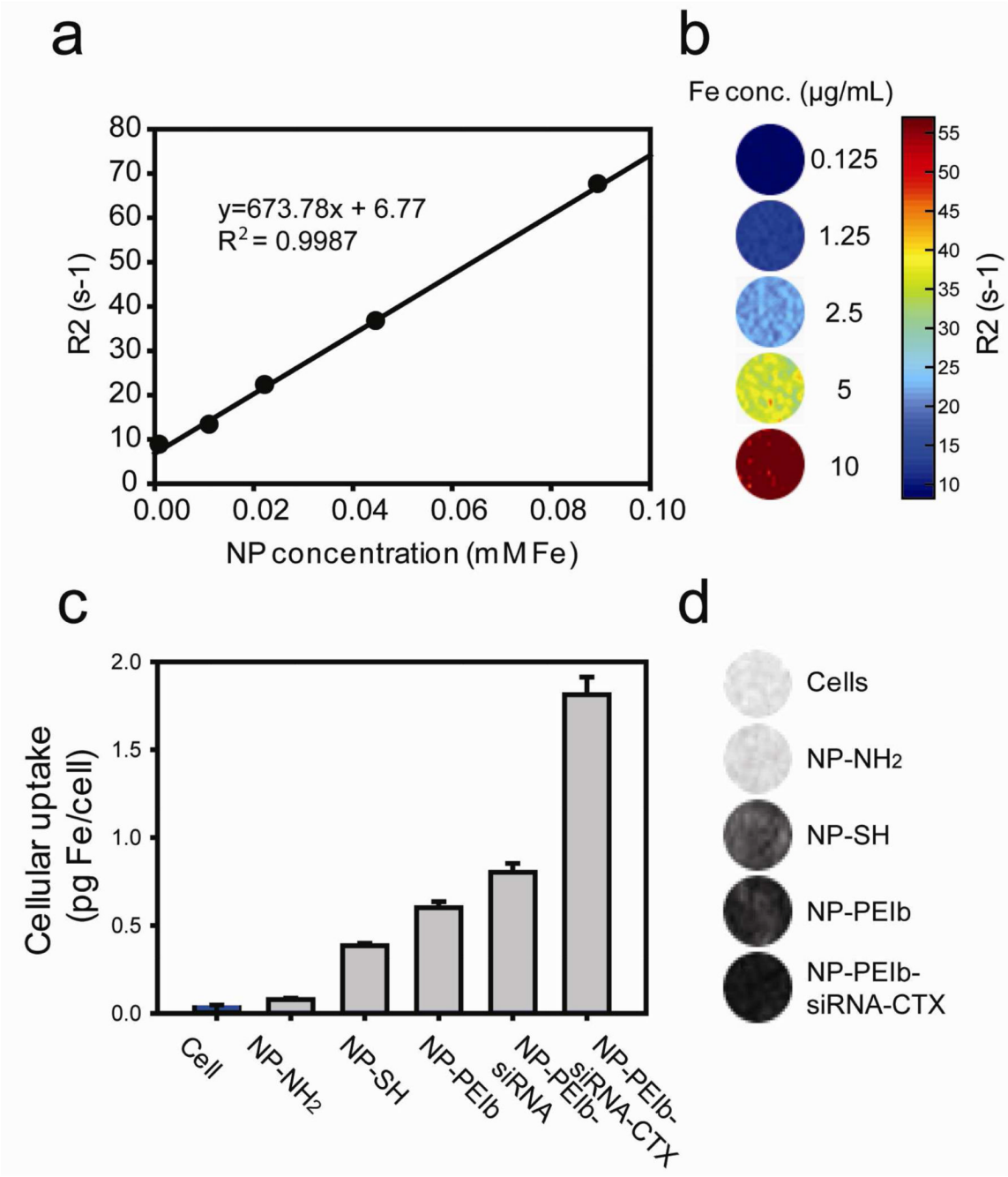

Figure 5.

Magnetic property of NP-PEIb-siRNA-CTX and cellular uptake of various nanoparticles. (a) R2 relaxation as a function of Fe concentration for NP-PEIb-siRNA-CTX. (b) R2 maps of gel phantoms containing NP-PEIb-siRNA-CTX at different Fe concentrations. (c) Intracellular uptake of different nanoparticles by C6 cells in terms of Fe content determined by the colorimetric ferrozine-based assay. All nanoparticles were treated with cells at pH 6.4 at a Fe concentration of 4 μg/mL. (d) R2 maps of gel phantoms containing cells treated with different nanoparticles. All cells were treated with nanoparticles at a concentration of 20 μg/mL.

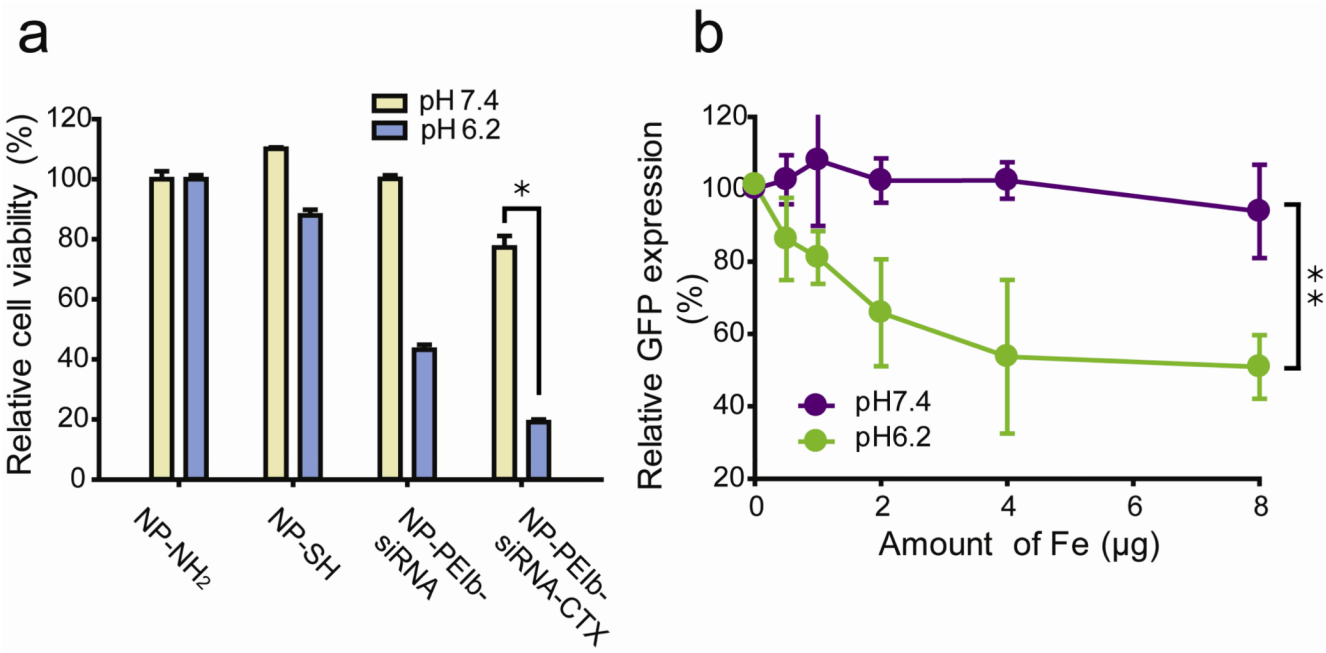

Figure 6.

Cytotoxic and gene silencing effects of various nanoparticles in C6 cells at pH 7.4 and pH 6.2. (a) Relative cell viability after cells were incubated with four different types of NPs for 48 hrs at a Fe concentration of 4 μg/well in serum-containing medium. (b) Relative GFP expression by cells treated with NP-PEIb-siRNA-CTX at various Fe concentrations, showing gene silencing effect. *p = 0.0001,**p < 0.002.